[논 문] 한국재료학회지
Korean J. Mater. Res.
Vol. 28, No. 1 (2018)
https://doi.org/10.3740/MRSK.2018.28.1.68

Bimetallic Co/Zn-ZIF as an Efficient Photocatalyst for Degradation of Indigo Carmine

Thanh Nhan Nguyen[1], Hoang Phuc Nguyen[1], Tae-Ho Kim[1†] and Soo Wohn Lee[2†]

[1]Research Center for Eco Multi-Functional Nano Materials, Sun Moon University, Asan, Chungnam 31460, Republic of Korea
[2]Department of Environmental and Bio-Chemical Engineering, Sun Moon University, Asan, Chungnam 31460, Republic of Korea

(Received August 28, 2017 : Revised November 29, 2017 : Accepted December 22, 2017)

Abstract Cobalt-incorporated zeolitic imidazolate framework ZIF-8 was synthesized by a simple one-pot synthesis method at room temperature. Powder X-ray diffraction patterns and energy dispersive X-ray spectrum confirmed the formation of the bimetallic Co/Zn-ZIF structure. UV-Vis diffuse reflectance spectra revealed that the bimetallic ZIF had a lower HOMO-LUMO gap compared with ZIF-8 due to the charge transfer process from organic ligands to cobalt centers. A hydrolytic stability test showed that Co/Zn-ZIF is very robust in aqueous solution - the most important criterion for any material to be applied in photodegradation. The photocatalytic efficiency of the synthesized samples was investigated over the Indigo Carmine (IC) dye degradation under solar simulated irradiation. Cobalt incorporated ZIF-8 exhibited high efficiency over a wide range of pH and initial concentration. The degradation followed through three distinct stages: a slow initial stage, followed by an accelerated stage and completed with a decelerated stage. Moreover, the photocatalytic performance of the synthesized samples was highly improved in alkaline environment rather than in acidic or neutral environments, which may have been because in high pH medium, the increased concentration of hydroxyl ion facilitated the formation of hydroxyl radicals, a reactive species responsible for the breaking of the Indigo Carmine structure. Thus, Co/Zn-ZIF is a promising and green material for solving the environmental pollution caused by textile industries.

Key words metal organic framework, bimetallic zeolitic imidazolate framework, indigo carmine, photodegradation.

1. Introduction

Indigo Carmine(IC) is a dark blue-purple colored dye of indigoid class.[1)] It is widely used in textile industries in an excessive amount for dyeing of polyester fibers and denim. However, this process is not very efficient since only around 70 % of applied dyes is used while the rest of the dye ends up discharging into the environment.[2)] This source of wastewater is causing pollution to the environment, having an adverse impact on the photosynthesis process of the subaqueous system since light penetration is obstructed in the system.[3)] Moreover, IC is highly toxic and contacting this chemical can cause skin and eye irritations, permanent injury to the cornea and conjunctiva. In addition, it leads to reproductive, developmental, neuro disorders as well as acute toxicity.[1)] To avoid these adverse impacts, a great deal of effort is required to develop green technologies for the removal of such pollutants in industrial wastewater.[4)]

Various techniques have been developed for the removal of IC from dye effluents. For the purpose of removing dye pollutants, conventional physical methods like adsorption were employed efficiently.[1,5)] However, these techniques are non-destructive, and the transfer of the pollutant from one phase to another causes secondary pollution which might be more serious than the primary. Moreover, post-treatment of the adsorbent material costs energy and was found to be a complicated process in some cases.[6)] Electrochemical degradation[4,7)] and electrocoagulation[3)] have also been applied but they also require

†Corresponding author
E-Mail : swlee@sunmoon.ac.kr (S. W. Lee, Sun Moon Univ.)
snowman@sunmoon.ac.kr (T. H. Kim, SunMoon Univ.)

a huge amount of energy. Similarly, chemical oxidative degradation has also been utilized[8] but it has high operating cost and limited effect on carbon content.[6] Photocatalysis by semiconductor catalysts is found to be an efficient technique in degrading organic pollutants.[9-12] However, the easy agglomeration and low solar energy conversion efficiency of these catalysts limit their application.[13] Thus, developing a novel catalyst has attracted great attention among the science community.

Metal-organic frameworks(MOFs) are hybrid, porous materials made from inorganic nodes(metal or cluster) and organic linkers. The linkers can be bi-, tri-, or tetratopic. MOF networks can, in principle, extend infinitely into one-, two-, or three-dimension.[14] Owing to their structural regularity and synthetic tunability, MOFs provide a platform to organize photosensitizers and catalytic centers in a single structure for effective conversion of solar energy. Moreover, the porous structure facilitates the diffusion of substrates and products through channels.[15] It is also worth mentioning that since the wavelength of UV and visible light is much larger than the pore diameter of MOFs, the light is not scattered by the pores. Hence, light penetration and scattering do not seem to be a big issue in MOFs.[16]

ZIF-8 is a kind of MOF constructed from 2-methylimidazole as organic linkers and zinc ions as inorganic nodes. It is chemically and thermally stable enough to survive in harsh catalytic conditions,[14,15] but the HOMO-LUMO gap is very large (5.16 eV)[17] which makes it infeasible for the photocatalytic application. ZIF-67 is another kind of MOF constructed from 2-methylimidazole and cobalt (II) ions, and it adopts similar crystal structure of ZIF-8.[18-20] Different from ZIF-8, ZIF-67 has a smaller HOMO-LUMO gap which favors light harvesting process,[20] but the low chemical stability limits its application. Herein, we combined ZIF-8 and ZIF-67 into a single structure for photocatalytic degradation of industrial wastewater. A single one-pot synthesis technique has been utilized to synthesize the samples. Photocatalytic properties were investigated with reference to IC dye as a model pollutant.

2. Experimental procedure

2.1 Materials

Zinc nitrate hexahydrate $Zn(NO_3)_2 \cdot 6H_2O$ (98 % purity) was purchased from Sigma-Aldrich Chemical Co. 2-methylimidazole (99 % purity) was purchased from Acros Organic Chemical Co. Cobalt nitrate hexahydrate $Co(NO_3)_2 \cdot 6H_2O$ (98 % purity) and Indigo Carmine were purchased from Alfa Aesar Chemicals Co. Hydrochloric acid (35-37 %) was purchased from Ducksan Chemical Co. Sodium hydroxide (98 % purity) was purchased from Samchun Chemical Co. All chemicals were used without further purification. Double distilled water was used where necessary.

2.2 Synthesis of photocatalyst

ZIF-8 was synthesized with slight modification to a previously reported procedure.[21] Specifically, $Zn(NO_3)_2 \cdot 6H_2O$ (3 mmol) was dissolved in 30 mL of methanol (MeOH) to form a clear solution, which was subsequently poured into 10 mL of MeOH containing 2-methylimidazole (12 mmol). After thorough mixing, the resulting solution was incubated at room temperature for 24 h. The as-obtained precipitates were centrifuged and washed with ethanol several times and dried at 80 °C for 12 h.

The similar procedure was followed to synthesize ZIF-67 and bimetallic ZIF with a small change in the metal source. In ZIF-67, the metal source was $Co(NO_3)_2 \cdot 6H_2O$ (3 mmol), while in bimetallic ZIF, the source was a mixture of $Co(NO_3)_2 \cdot 6H_2O$ (0.6 mmol) and $Zn(NO_3)_2 \cdot 6H_2O$ (2.4 mmol).

2.3 Characterization

The crystallinity of samples was investigated by X-ray diffraction spectroscopy. The spectra were recorded from 2° to 40° of 2θ on XRD spectrometer(Rigaku D/max-2200 HR) with Cu Kα ($\lambda = 1.54$ Å) radiation at a scan rate of 4°/min with a step size of 0.02°. The morphology of samples was observed by scanning electron microscopy (SEM, Nano-eye, SNE 2000 M). Chemical composition was analyzed with energy dispersive X-ray spectroscopy (EDS, Oxford Instruments X-Max^N 50) combined with Field-emission scanning electron microscopy(FE-SEM, JSM-6700F). The chemical structure of samples was investigated by Fourier transform infrared spectroscopy (FT-IR, Vertex 70(Bruker)) in the range of 4000-650 cm^{-1}. UV-Vis absorption of samples was collected on UV-Vis diffuse reflectance spectrophotometer(JASCO-V 570 spectrophotometer), and $BaSO_4$ was used as reference material. The surface area of samples was obtained from N_2 adsorption-desorption isotherms at 77 K using Brunauer-Emmett-Teller(BET) method(ASAP 2020 Micrometrics Instrument Corporation). Before the sorption experiment, the samples were activated at 150 °C under vacuum for 10 h. The change in dye absorbance was monitored with a double beam UV-Vis spectrophotometer(Mega-2100) in the range of 450-700 nm in a 1 cm path length spectrometric quartz cell, and the IC concentration was estimated by the absorbance at 610 nm. The light source for the photocatalytic reaction was obtained from a solar simulator using 150 W short arc lamp.

2.4 Test for hydrolytic stability

To test the hydrolytic stability, 100 mg of powder

sample was dispersed in 30 ml of distilled water and kept in dark. After every 24 h, 3 ml of dispersed solution was taken out and mixed with ethanol in the ratio water: ethanol = 1:10 and centrifuged before drying in an oven at 80 °C for 12 h. Dried samples were tested for the integrity of chemical structure via the FT-IR measurement.

2.5 Photocatalytic test

Photocatalytic activity of the prepared sample was evaluated by IC dye degradation in aqueous medium under solar simulated irradiation. The initial dye concentration(C_0) was 50 ppm. Before turning on the light, the solution containing dye and photocatalyst was stirred using a magnetic stirrer in a dark condition for 90 min in order to establish the absorption-desorption equilibrium. Then, the solution was irradiated by solar simulator at constant stirring speed. Sample portions of 1 mL were extracted from the reactor every 20 min using a syringe filter. Samples were tested with UV-Vis absorption.

3. Results and discussion

3.1 Properties of Co/Zn-ZIF

The synthesized sample has characteristic violet color as shown in Fig. 1. The color results from the tetrahedral-coordinated cobalt. EDS measurement was conducted on cobalt-doped ZIF-8 to confirm the presence of cobalt (Fig. 2). The practical value of Co/Zn molar ratios within the bimetallic ZIFs (19:81) is approximately equal to the theoretical value (20:80).

Fig. 3 shows typical XRD patterns for the ZIF-8, ZIF-67 and Co/Zn-ZIF. Co/Zn-ZIF displayed very sharp peaks analogous to those of ZIF-8 and ZIF-67, indicating that Co/Zn-ZIF adopted the same crystalline structure of single-metal ZIFs with cubic unit cell in the $I\bar{4}3m$ space group.[22] This can be explained that ZIF-8 and ZIF-67 have the same topology(sod),[18] similar bond lengths and atomic radii as well as cell parameters which enable the unlimited solubilility of Co phase in the Zn phase and vice versa.[22] All patterns show sharp peaks, no additional phase was found, indicating that the as-synthesized samples have a high purity and crystallinity. The slight difference in bond length of Co-N(1.976 Å) and Zn-N(1.987 Å) induced certain local distortions and related stress in the network[22] which broadened the peaks of Co/Zn-ZIF. It is also interesting that there was a slight but systematic shift of Co/Zn-ZIF peaks towards lower 2θ with respect to ZIF-8. The inset in Fig. 3 illustrates this shift with the (211) peak. This supports the incorporation of cobalt in ZIF-8 framework.[20]

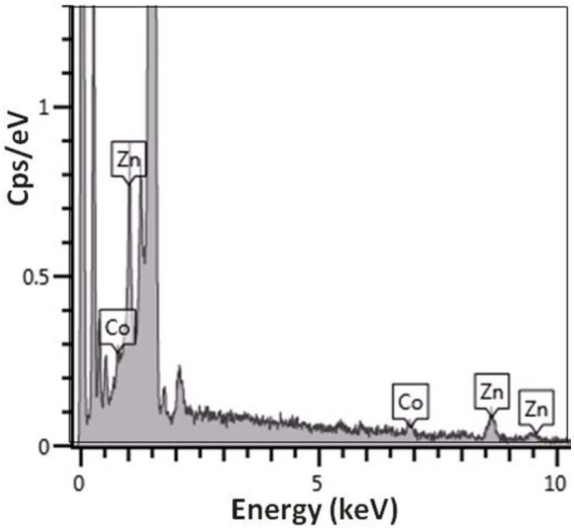

Fig. 2. Energy-dispersive X-ray spectrum of Co/Zn-ZIF.

Fig. 4 shows SEM images of ZIF-8, Co/Zn-ZIF and ZIF-67. As can be obviously seen, Co/Zn-ZIF preserved the typical rhombic dodecahedral morphology of single metal ZIFs and had good uniformity with an average size of approximately 0.5 μm. Compared with ZIF-67 and ZIF-8, Co/Zn-ZIF crystal was smaller in size, which was caused by the stress in the network. As mentioned above, Co-N and Zn-N are different in bond length. Hence, when Co and Zn were incorporated in the same ZIF crystal, local distortion and stress appeared which hindered the crystals growth, resulting in powder of smaller crystal size.[22]

Light absorption of Co/Zn-ZIF was compared with that

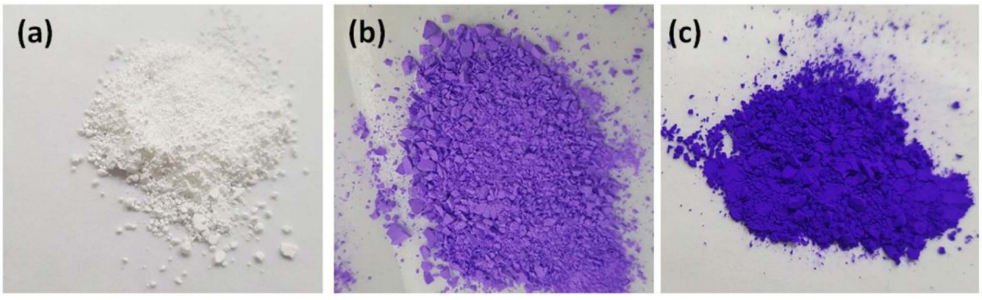

Fig. 1. Optical photographs of (a) ZIF-8, (b) Co/Zn-ZIF, and (c) ZIF-67 powder taken in visible light.

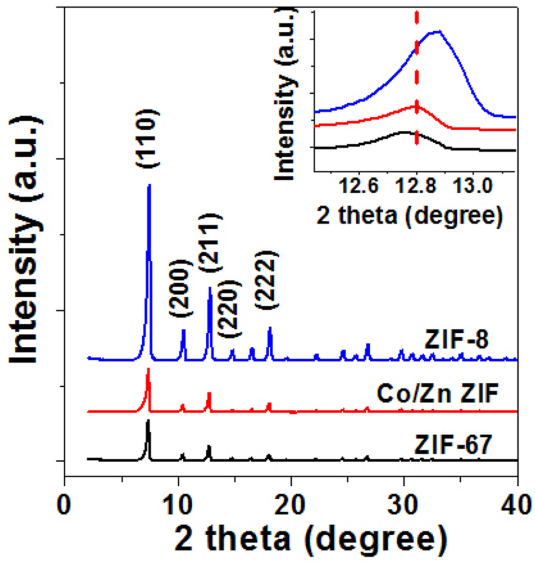

Fig. 3. XRD patterns for ZIF-8(blue), Co/Zn-ZIF(red), and ZIF-67 (black). The inset illustrates the shift of the (211) peak of Co/Zn-ZIF.

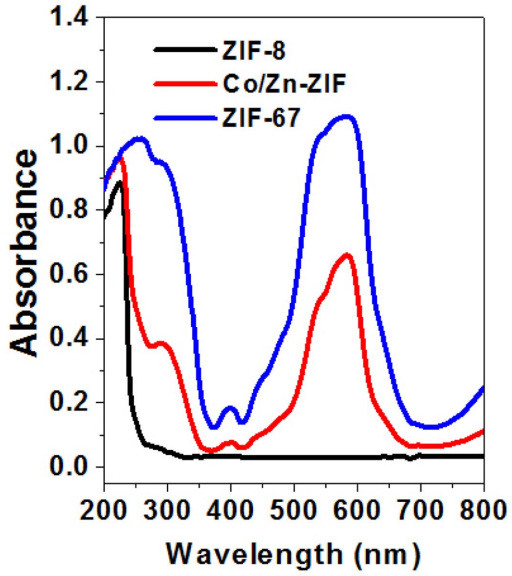

Fig. 5. UV-Vis diffuse reflectance spectra of ZIF-8, Co/Zn-ZIF and ZIF-67.

of ZIF-67 and ZIF-8(Fig. 5). It is clearly observed that while ZIF-8 only show an absorption at < 250 nm due to π-π* transition located in organic ligand, ZIF-67 and Co/Zn-ZIF show an intense characteristic absorption band from 450-650 nm, which is assigned for the typical [$^4A_2$(F)-$^4T_1$(P)] d-d transition in tetrahedral cobalt. An absorption in UV region extended to 350 nm, which is caused by the ligand-to-metal charge transfer(LMCT) process.[23] The specific surface area of Co/Zn-ZIF was investigated by using the nitrogen adsorption-desorption isotherms at 77 K using Brunauer-Emmett-Teller(BET) theory(Fig. 6). Co/Zn-ZIF sample showed Type I isotherms with a surface area of 1513(m^2/g), similar with that of ZIF-8 and ZIF-67(1554 and 1503 m^2/g respectively). Moreover, Co/Zn-ZIF showed fast adsorption and reached a saturation level at relative pressure < 0.05, indicating that material is microporous, analogous to single-metal ZIFs.

3.2 Hydrolytic stability

The greatest concern for MOF's chemical stability is largely related to water. In most MOF structures, the chemically weak points are at the nodes. More specifically, when contacting with water, the metal-linker bonds hydrolyze, yielding a protonated linker and a hydroxide(or water) ligated node.[14] To check for water stability, FT-IR was utilized to detect the presence of the hydroxyl group in our samples. The data of Co/Zn-ZIF is shown in Fig. 7(b), together with ZIF-8 and ZIF-67(Fig. 7(a) and 7(c)) for better comparison. ZIF-8 is well-known for its chemical stability, so it is not surprising that it remained intact after 120 h. All the characteristic peaks remained unchanged and no additional peaks appeared. The peaks at 991 and 1142 cm^{-1} were assigned to C-N stretching mode,[17] the characteristic peak at 1585 cm^{-1} was due to C=N stretching, whereas bands between 1350-1500 cm^{-1} can be assigned to the entire ring stretching.[24] Unlike ZIF-8, ZIF-67 was vulnerable in water and showed a sharp peak at 3630 cm^{-1} after 24 h of immersing in water which is assigned to hydroxide group. This implied that the link between cobalt and ligand in ZIF-67 is not very stable in water. Surprisingly, Co/Zn-ZIF preserved its chemical structure after 120 h of soaking

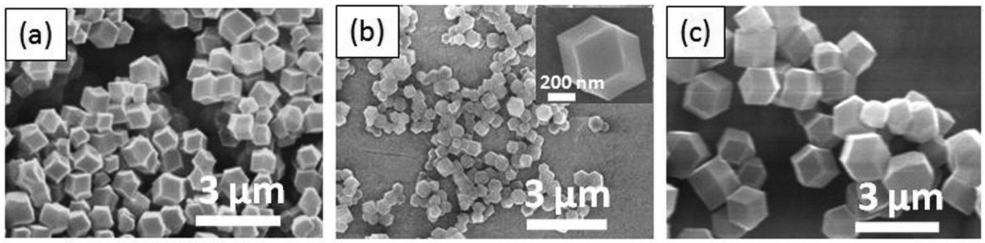

Fig. 4. SEM images of (a) ZIF-8, (b) Co/Zn-ZIF, and (c) ZIF-67.

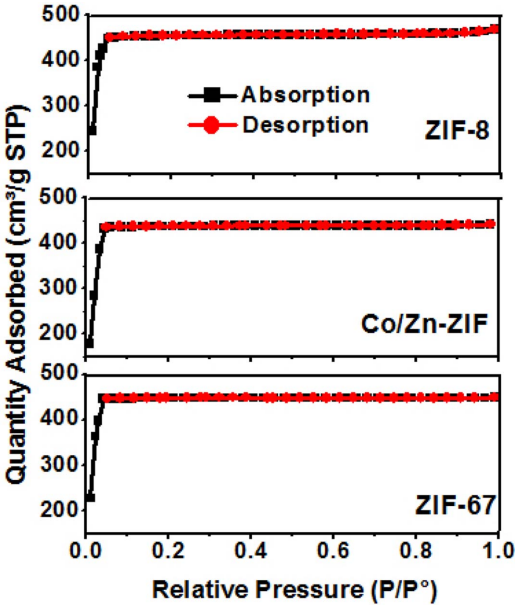

Fig. 6. Nitrogen sorption isotherms of ZIF-8, Co/Zn-ZIF, and ZIF-67.

in water, which was comparable with ZIF-8. It is concluded that the presence of zinc helped stabilize Co/Zn-ZIF structure. Thus, Co/Zn-ZIF is a potential candidate for applications in aqueous solution.

3.3 Photocatalytic activity of Co/Zn-ZIF

The photocatalytic degradation of IC was conducted to evaluate the efficiency of the Co/Zn-ZIF material. In every experiment, the Co/Zn-ZIF amount was kept constant (0.2 g/L). The UV-Vis absorption spectra of the undecomposed IC during the photodegradation reaction are illustrated in Fig. 8(a) and 8(b), indicating that the concentration of IC decreased over time under the photocatalytic activity of Co/Zn-ZIF. Interestingly, photocatalytic degradation showed three distinct stages: very slow reaction rate initially (13 % within 80 min), a fast reaction rate in the next stage (47 % within the next 80 min) and finally decelerated reaction rate at the last stage. This result is different from previous works of IC photodegradation catalyzed by other materials in which the rate reduced by time due to the reduction of dye concentration.[10-12,25] This can be explained that because adsorption capacity of Co/Zn-ZIF was relatively high, dye molecules formed a thick layer on the surface of the catalyst in the first stage. This layer covered the active sites and prevented the catalyst from absorbing photons. Also at this stage, catalyst mainly decomposed dye

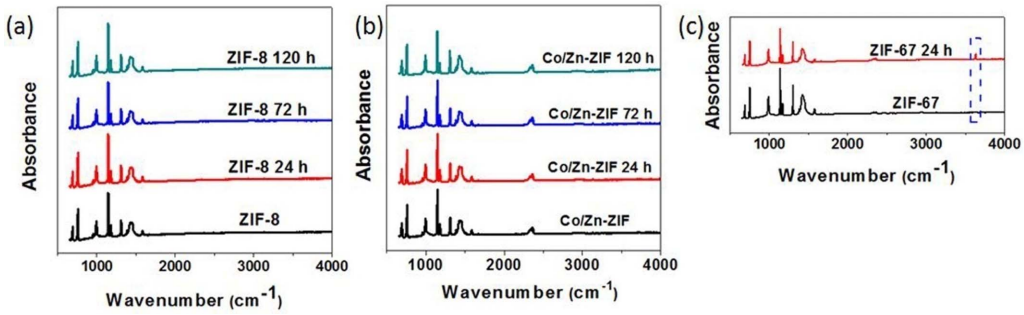

Fig. 7. FT-IR spectra of (a) ZIF-8, (b) Co/Zn-ZIF, and (c) ZIF-67 dry powder after soaking in water.

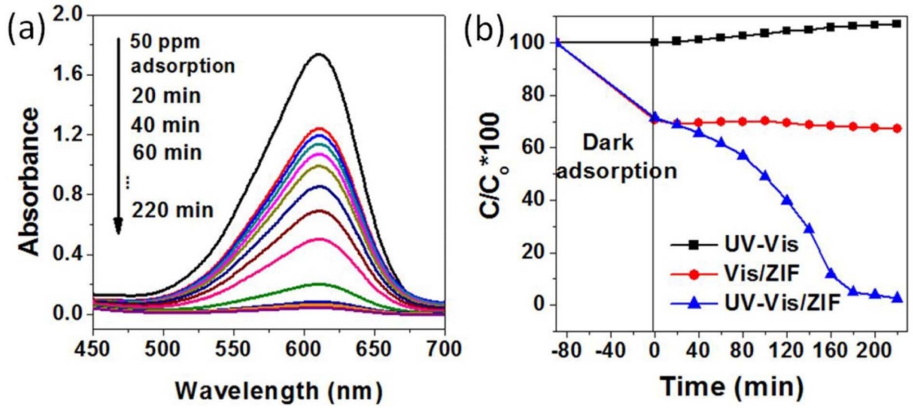

Fig. 8. (a) UV-Vis absorption spectra of IC solution during decomposition reaction under solar simulated irradiation in the presence of Co/Zn-ZIF, (b) degradation of IC under different conditions, initial pH of solutions is 5.

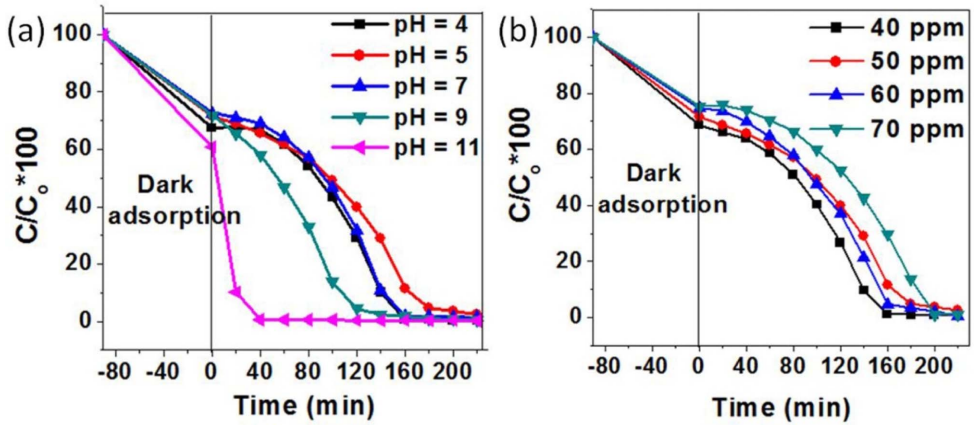

Fig. 9. (a) Effect of pH and (b) effect of initial concentration on the degradation of dye.

adsorbed on the surface rather than dye in water solution. Hence, dye concentration did not change significantly. After a while, the dye layer on the surface was degraded, allowing the catalyst to absorb photon effectively. Also, IC in the solution came into contact with the catalyst and was degraded. Thus, the degradation rate at the middle stage was relatively fast. At the last stage, dye concentration was low so the interaction between dye and catalyst was not favorable. Moreover, the incomplete degradation products may adsorb on the catalyst surface and compete with IC. After 3 h, nearly 100 % of IC was photocatalytically decomposed. When the experiment was carried out only in visible light(UV cut off ≥ 420 nm), Co/Zn-ZIF did not show any photocatalytic effect on IC, (Fig. 8(b)) which indicated that the d-d transition of electron did not create reactive species for the degradation of IC. Hence, the proposed mechanism is that when Co/Zn-ZIF absorbed photons with wavelength lower than 350 nm, the charge transfer takes place from HOMO (mostly contributed by nitrogen 2p bonding orbital) to LUMO(mostly contributed by Co empty orbital),[13] creating a hole in organic ligand and a reactive electron in cobalt metal center. This electron-hole pair then reacted with the dissolved oxygen and water to produce reactive oxygen species(ROS) such as hydroxyl radicals ($OH^{\cdot -}$), superoxide($O_2^{\cdot -}$), singlet oxygen($^1O_2$), and peroxide(H_2O_2) and then those ROS species broke the IC structure into simpler compounds.[26]

3.3.1 Effect of initial pH and initial dye concentration

The pH of dye solution is a crucial factor influencing the photocatalytic degradation.[17] In order to determine the effect of pH on degradation process, five solutions of different pH(4, 5, 7, 9, 11) were prepared. The pH was adjusted by 0.1 M solution of HCl and NaOH and the data were illustrated in Fig. 9(a). The results revealed that Co/Zn-ZIF can work effectively over a wide pH range from 4 to 11, and the photocatalytic ability improved with the increase of pH. This may be explained that at high pH environment, the concentration of hydroxyl ions was high, facilitating the formation of hydroxyl radicals.[27] When pH of the solution increased to 11, Co/Zn-ZIF showed higher adsorption capacity and very fast degradation rate for IC.

The influence of initial dye concentration on the degradation of IC was investigated. Four different solutions with dye concentration ranged from 40 ppm to 70 ppm (with the gap of 10 ppm) were prepared and the results were illustrated in Fig. 9(b). As the initial dye concentration increased, the time period required for the complete degradation process also increased. At high concentration, more light was blocked from penetrating into water, which disables light absorption of the catalyst to generate electron-hole pairs.[27]

4. Conclusions

Bimetallic Co/Zn-ZIF was synthesized by a simple and straightforward methodology. The materials were characterized by XRD, SEM, FE-SEM-EDS, UV-Vis diffuse reflectance spectroscopy, and BET measurement. The results confirmed the successful incorporation of cobalt into ZIF-8 structure. The hydrolytic stability test proved that Co/Zn-ZIF is highly stable in water, making it suitable for applications in aqueous medium. Moreover, due to the incorporation of cobalt in the catalyst, the material can take advantage of the broad adsorption of LMCT bands. Photodegradation experiments showed that Co/Zn-ZIF is an efficient photocatalyst for degradation of IC under solar light irradiation with almost 100 % removal in less than 3 h. This photocatalytic degradation started with a very slow stage, followed by an accelerated stage and finally the rate decelerated until all dye was removed completely from the solution. Co/Zn-ZIF worked effect-

ively over a wide range of initial concentration. pH of the solution was found to be an important parameter, greatly influenced the degradation rate. Especially, Co/Zn-ZIF had very good catalysis performance in strong alkaline medium. Thus, bimetallic Co/Zn-ZIF could be considered as a potential candidate for photodegradation of organic pollutants from textile industries.

Acknowledgement

This research was supported by Global Research Laboratory Program of the National Research Foundation of Korea(NRF) funded by the Ministry of Education, Science and Technology(MEST) of Korea(Grant No.: 2010-00339) and Basic Science Research Program through the National Research Foundation of Korea(NRF) funded by the Ministry of Science, ICT and Future Planning (NRF-2015R1C1A1A01052893).

References

1. A. Mittal, J. Mittal and L. Kurup, J. Hazard. Mater., **137**, 591 (2006).
2. E. Gutiérrez-Segura, M. Solache-Ríos and A. Colín-Cruz, J. Hazard. Mater., **170**, 1227 (2009).
3. M. S. Secula, I. Crežescu and S. Petrescu, Desalination, **277**, 227 (2011).
4. S. Ammar, R. Abdelhedi, C. Flox, C. Arias and E. Brillas, Environ. Chem. Lett., **4**, 229 (2006).
5. S. M. de Oliveira Brito, H. M. C. Andrade, L. F. Soares and R. P. de Azevedo, J. Hazard. Mater., **174**, 84 (2010).
6. I. K. Konstantinou and T. A. Albanis, Appl. Catal. B, **49**, 1 (2004).
7. C. Flox, S. Ammar, C. Arias, E. Brillas, A. V. Vargas-Zavala and R. Abdelhedi, Appl. Catal. B, **67**, 93 (2006).
8. P. Jackson and M. I. Attalla, Rapid Commun. Mass Spectrom., **21**, 1893 (2007).
9. A. G. S. Prado, L. B. Bolzon, C. P. Pedroso, A. O. Moura and L. L. Costa, Appl. Catal. B, **82**, 219 (2008).
10. M. Vautier, C. Guillard and J-M. Herrmann, J. Catal., **201**, 46 (2001).
11. N. Barka, A. Assabbane, A. Nounah and Y. A. Ichou, J. Hazard. Mater., **152**, 1054 (2008).
12. J. D. Torres, E. A. Faria, J. R. SouzaDe and A. G. S. Prado, J. Photochem. Photobiol. A, **182**, 202 (2006).
13. C. Wang, J. Li, X. Lv, Y. Zhang and G. Guo, Energy Environ. Sci., **7**, 2831, (2014).
14. A. J. Howarth, Y. Liu, P. Li, Z. Li , T. C. Wang , J. T. Hupp and O. K. Farha, Nat. Rev. Mater., **1**, 1 (2016).
15. T. Zhang and W. Lin, Chem. Soc. Rev., **43**, 5982 (2014).
16. M. A. Nasalevich, M. van der Veen, F. Kapteijn and J. Gascon., CrystEngComm., **16**, 4919 (2014).
17. H-P. Jing, C-C. Wang, Y-W. Zhang, P. Wang and R. Li, RSC Adv., **4**, 54454 (2014).
18. K. Zhou, B. Mousavi, Z. Luo, S. Phatanasri, S. Chaemchuen and F. Verpoort, J. Mater. Chem. A, **5**, 952 (2017).
19. J. K. Zaręba, M. Nyk and M. Samoc, Cryst. Growth Des., **16**, 6419 (2016).
20. G. Kaur, R. K. Rai, D. Tyagi, X. Yao, P-Z. Li, X-C. Yang, Y. Zhao, Q. Xu and S. K. Singh, J. Mater. Chem. A, **4**, 14932 (2016).
21. R. Wu, X. Qian, K. Zhou, J. Wei, J. Lou and P. M. Ajayan, ACS Nano, **8**, 6297 (2014).
22. C. Sámano-Alonso, J. Hernández-Obregón, R. Cabrera, J.A.I. Díaz-Góngora and E. Reguera, Colloids Surf. A: Physicochem. Eng. Aspects. **506**, 50 (2016).
23. B. Pattengale, S. Yang, J. Ludwig, Z. Huang, X. Zhang and J. Huang, J. Am. Chem. Soc., **138**, 8072 (2016).
24. E. L. Bustamante, J. L. Fernández and J. M. Zamaro, J. Colloid Interface Sci., **424**, 37 (2014).
25. L. L. Costa and A. G. S. Prado, J. Photochem. Photobiol. A, **201**, 45 (2009).
26. Y. Qu, X. Zhong, Y. Li, L. Liao, Y. Huang and X. Duan, J. Mater. Chem., **20**, 3590 (2010).
27. L. S. Reddy Yadav, K. Lingaraju, K. Manjunath, G. K. Raghu, K. H. Sudheer Kumar and G. Nagaraju, Mater. Res. Express, **4**, 1 (2017).